Seeded Semibatch Emulsion Copolymerization of n-Butyl Acrylate and Methyl Methacrylate

ARTICLE *in* INDUSTRIAL & ENGINEERING CHEMISTRY RESEARCH · SEPTEMBER 2004

Impact Factor: 2.59 · DOI: 10.1021/ie0400649

4 AUTHORS, INCLUDING:

Oihana Elizalde
BASF SE
13 PUBLICATIONS **255** CITATIONS
SEE PROFILE

Jose R Leiza
Universidad del País Vasco / Euskal Herriko U…
145 PUBLICATIONS **2,585** CITATIONS
SEE PROFILE

Seeded Semibatch Emulsion Copolymerization of *n*-Butyl Acrylate and Methyl Methacrylate

Oihana Elizalde,[†] Gurutze Arzamendi,[‡] Jose R. Leiza,*[,†] and Jose M. Asua[†]

Institute for Polymer Materials, POLYMAT, and Grupo de Ingeniería Química, Departamento de Química Aplicada, Facultad de Ciencias Químicas, The University of the Basque Country, Apartado 1072, 20080 Donostia-San Sebastián, Spain, and Departamento de Química Aplicada, Universidad Pública de Navarra, 31006 Pamplona, Spain

The kinetics and polymer microstructure of the seeded semibatch emulsion copolymerization of *n*-BA/MMA were investigated in this work. Free monomer concentration was determined on-line by means of FT-Raman spectrosocopy. The kinetics, gel fraction, and molecular weight distribution were determined for several semibatch reactions of different monomer composition. The experiments show that, when the amount of MMA in the recipe was increased (from 90/10 to 50/50 *n*-BA/MMA by moles), the instantaneous conversion increased, whereas the gel content decreased and the sol molecular weight exhibited no defined trend. A mathematical model was used to analyze the experimental data.

Introduction

Emulsion polymerization is a versatile technique, widely used in industry to produce latexes for a large variety of applications including paints, coatings, adhesives, and binders in the textiles and paper industries.[1] Acrylics are a family of emulsion polymers extensively used in industry, with *n*-butyl acrylate/methyl methacrylate (*n*-BA/MMA) being one of the most commonly used monomer systems. This comonomer system is extremely versatile, and depending on the weight ratio between the comonomers, latexes used for very different applications can be produced. Typically, copolymers with a 50/50 wt/wt *n*-BA/MMA composition are used for coatings, and those with at least of 90 wt % of *n*-BA are used as adhesives.

The end-use properties of these latexes depend on the microstructural properties of the polymer; therefore, to meet the increasing demands on product quality, the structural properties of the polymer should be controlled. To achieve this control, it is important to understand the fundamental physicochemical phenomena involved in the emulsion copolymerization of *n*-BA and MMA. An important aspect of this monomer system is that a gel can be formed, and the gel fraction strongly affects the final properties of the product. To develop proper control strategies, a mathematical model able to describe the copolymerization kinetics and the evolution of the aforementioned polymer properties should be used.

Dubé and Penlidis[2] studied the conversion, molecular weight, composition, and particle size of *n*-BA/MMA emulsion copolymerizations, but they did not report results regarding the gel fraction. Chern and Hsu[3] studied the semibatch emulsion copolymerization of *n*-BA/MMA, focusing on the effects of various reaction parameters on the particle nucleation and growth. Novak[4] presented a model to describe particle nucleation and growth during semibatch emulsion copolymerizations of *n*-BA/MMA. Ouzineb et al.[5] carried out emulsion homopolymerizations and copolymerizations of *n*-BA and MMA with different types and concentrations of surfactants to investigate the mechanism of particle formation. Britton et al.[6] observed that the level of branches in *n*-BA polymerizations was reduced by the introduction of MMA as a comonomer. The reason for this decrease in branching is that MMA gives rise to both polymeric radicals with lower chain-transfer reactivity and monomeric units in the polymer chains that do not have abstractable tertiary hydrogens. In none of these works were the kinetics, composition, sol molecular weight distribution (MWD), and gel fraction of the *n*-BA/MMA comonomer system studied simultaneously.

Sayer et al.[7] studied the effect of a chain-transfer agent (CTA, dodecanethiol) on the kinetics and MWD of *n*-BA/MMA semibatch emulsion polymerizations at a fixed 50/50 molar composition. No substantial effect of the CTA on the kinetics was observed, but the MWD decreased with the CTA concentration, and a concentration of 1 wt % CTA was enough to avoid gel formation during the process. The same authors investigated the effects of different strategies for copolymer composition control on the sol MWD and gel fraction.[8] They observed that a starved process gave more gel and lower sol molecular weights than a semistarved process. Sayer et al.[7,8] measured the gel fraction as the relative difference between the concentration of the polymer injected into the gel permeation chromatography (GPC) column and the polymer concentration detected in the GPC analysis. However, comparison of this method with those based on extraction processes[9] showed that the GPC method was less reproducible and tended to overestimate the amount of gel.[10]

In the present work, the effects of the comonomer ratio on the kinetics of the high-solids-content, seeded semicontinuous emulsion copolymerization of *n*-BA/MMA and on the properties of the polymer produced were investigated. Such a study has not previously been reported in the open literature. The evolution of the copolymerization reactions was followed by conventional off-line characterization techniques and also by on-line

* To whom correspondence should be addressed. Tel.: +34 943015329. Fax: +34943015270. E-mail: jrleiza@sq.ehu.es.
[†] The University of the Basque Country.
[‡] Universidad Pública de Navarra.

10.1021/ie0400649 CCC: $27.50
Published on Web 09/25/2004

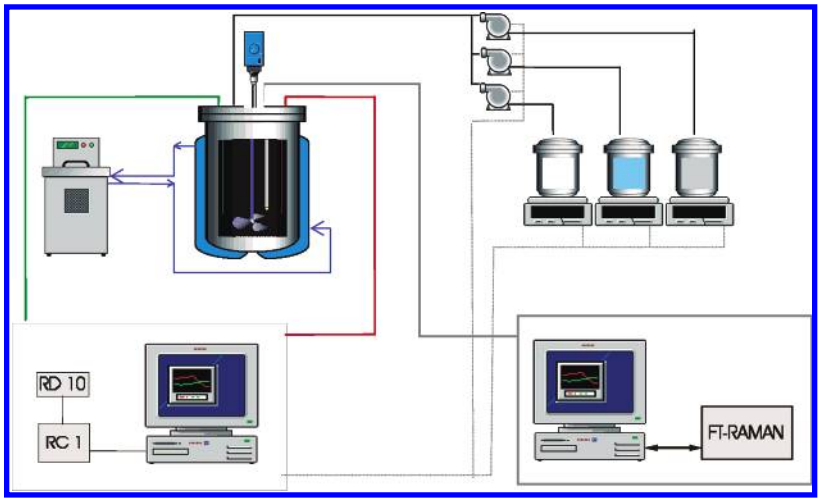

Figure 1. Scheme of the experimental setup used in this work.

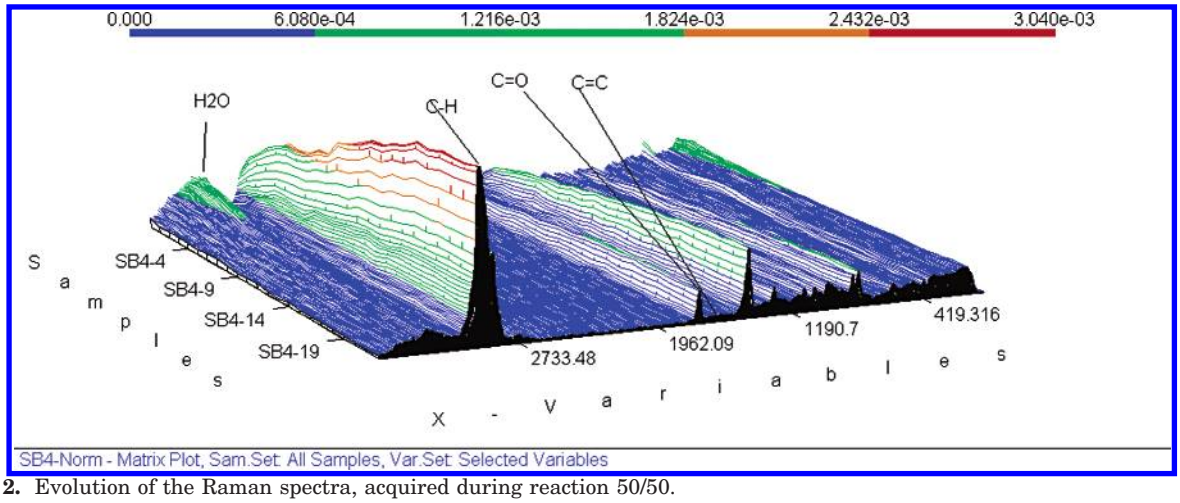

Figure 2. Evolution of the Raman spectra, acquired during reaction 50/50.

Fourier transform Raman spectroscopy (FT-Raman). Following Plessis et al.,[11] a mathematical model whose outputs include the evolution of the reaction kinetics, copolymer composition, sol MWD, and gel fraction was used to analyze the data.

Experimental Section

Materials. All reactants, monomers (*n*-BA and MMA, Quimidroga), emulsifier (Dowfax 2A1, Dow), initiator ($K_2S_2O_8$, Fluka), and buffer ($NaHCO_3$, Panreac) were used as supplied. The same initiator and emulsifier were used in the preparation of the seeds and in the seeded emulsion copolymerization reactions. All polymerizations were carried out using doubly deionized water and were performed in an inert N_2 atmosphere.

Experimental Setup. The experimental setup (schematically shown in Figure 1) employed to prepare the seeds and run the seeded reactions was a commercial calorimetric reactor (RC1, Mettler-Toledo) equipped with a stainless steel HP60 reactor with a capacity of 1.5 L. The reactor was also equipped with an FT-Raman dip probe that was directly immersed into the reaction mixture, enabling the in situ collection of spectra during the reaction.

The spectrometer used in the experiments was a near-infrared Fourier transform Raman (NIR FT-Raman) spectrometer, RFS 100/S (Bruker), equipped with a 1064-nm-wavelength Nd:YAG laser with a maximum power of 1.5 W. The spectral coverage was from 50 to 3500 cm^{-1}, corresponding to the Stokes interval. The spectrometer used a germanium detector (D481-TU) optimized for FT-Raman measurements that was cooled with liquid nitrogen. The Raman dip probe was connected to the equipment through two optical fibers (each 5 m long), one to carry the laser signal to the reaction mixture and the other to carry the scattered radiation back to the spectrometer. Raman spectra were collected from the start of the reaction at regular intervals of 10 min. Each spectrum consisted of the accumulation of 200 scans and was recorded with a spectral resolution of 4 cm^{-1} using a laser power of 1000 mW. The OPUS software (supplied with the instrument by Bruker) was used for data acquisition and preprocessing. Figure 2 shows the spectral evolution along the semicontinuous emulsion polymerization carried out at a monomer molar ratio of BA/MMA = 50/50.

The spectra were used to monitor the unreacted amounts of monomer in the reactor (*n*-BA and MMA) using appropriate calibration techniques as described elsewhere.[12]

The experimental setup was connected to two computers, one for the on-line acquisition and analysis of the Raman spectra and the other for monitoring of the evolution of the reaction (temperatures, agitation) and control of the pumps.

Table 1. Formulation of the Seeds[a]

component	amount (g)
H_2O	1080
KPS	0.4
$NaHCO_3$	0.4
n-BA + MMA	120[b]
Dowfax	varying

[a] Temperature = 80 °C. [b] Monomer ratio varied.

Table 2. Properties of the Seeds Prepared According to the Formulation in Table 1

seed	composition (molar, BA)	d_p[a] (nm)	$\overline{M_w}$ (g/mol)	$\overline{M_n}$ (g/mol)	gel (%)
S1	0.5	82	3.4×10^6	2.9×10^5	<1
S2	0.7	89	4.5×10^6	5.8×10^5	<1
S3	0.9	84	3.7×10^6	5.1×10^5	<1

[a] Dynamic light scattering (N4 Plus, Coulter).

Table 3. Formulation of the Seeded *n*-BA/MMA Emulsion Copolymerizations[a]

ingredient	initial charge (g)	stream 1 (g)	stream 2 (g)
n-BA + MMA	–	540[b]	–
H_2O	617	–	32.5
polymer seed	63	–	–
$K_2S_2O_8$[c]	2	–	–
$NaHCO_3$[c]	2	–	–
Dowfax	–	–	9.5

[a] Feeding time = 180 min. Temperature = 80 °C. [b] Monomer ratio varied. [c] One gram of each initator and emulsifier was used in the reaction BA/MMA = 50/50.

Polymerizations and Latex Characterization. All reactions performed in this study were seeded. The seeds were prepared in a batch reactor, according to the recipe shown in Table 1. In all cases, the final solids content of the seeds was 10 wt %, and the reaction temperature was 80 °C. The seeds were kept overnight at 90 °C in order to decompose the unreacted initiator. The properties of the seeds are summarized in Table 2. Three seeded semicontinuous emulsion polymerizations (at molar compositions of BA/MMA = 50/50, 70/30, and 90/10) were carried out in the experimental setup depicted in Figure 1, using the formulation in Table 3. In each reaction, a seed of the same comonomer composition as that employed in the reaction was used. All reactions were carried out at 70 °C, and the initial charge contained water, the corresponding seed, and the initiator. The monomer and emulsifier were fed along the reaction for 3 h. Constant flow rates were used for the monomers and the emulsifier.

(a) Global and Instantaneous Conversions. Samples withdrawn from the reactor were analyzed gravimetrically to calculate the overall conversion (based on the total amount of monomer in the formulation) and the instantaneous conversion (based on the total amount of monomer fed up to the sampling time).

(b) Residual Monomer and Cumulative Copolymer Composition. The amount of residual monomer in the reactor was measured with the Raman spectrometer, and the cumulative copolymer composition was measured by analyzing the latex samples with a gas chromatograph (GC) and applying material balances for the monomers. A gas chromatograph (Shimadzu GC-14A) with a flame ionization detector (FID) and an integrator (Shimadzu C-R6A) was used in this work.

(c) Gel Fraction. The gel fractions of the samples taken along the reaction were measured via conventional Soxhlet extraction, using tetrahydrofurane (THF) as the solvent. A glass fiber disk was impregnated with latex (a few drops), and the extraction was carried out for 8 h under reflux conditions (about 75 °C). The gel remained in the glass fiber, whereas the sol polymer was recovered from the THF solution. The amount of gel was calculated using the equation

$$\text{gel} = \frac{w_g}{w_p} \tag{1}$$

where w_g and w_p are the weights of the insoluble fraction and the whole polymer sample, respectively.

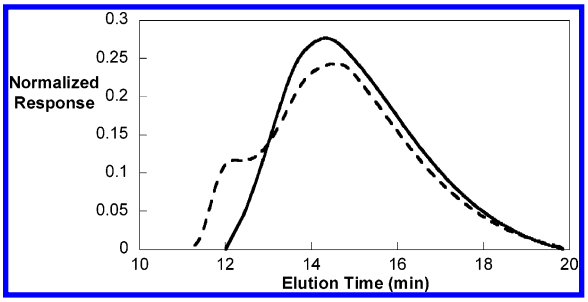

Figure 3. Normalized response versus elution time for a sample of reaction 90/10, measured on fraction collected from Soxhlet extraction (—) and from the direct dissolution of the latex (– – –).

(d) Molecular Weight Distribution. The molecular weight distribution and the average molecular weight of the soluble fraction were determined by gel permeation chromatography (GPC) at 35 °C. The GPC instrument consisted of an injector, a pump (Waters 510), three columns in series (Styragel HR2, HR4, and HR6), and a differential refractometer (Waters 2410) as the detector. The MWD of the samples was measured in two different ways. In the first, a few droplets of latex, as obtained from the reaction medium, were added to 2–3 mL of tetrahydrofuran (THF), the mixture was filtered, and the filtrate was injected into the GPC. In the second approach, the sol part obtained after Soxhlet extraction (see Gel Fraction section) was concentrated and then directly analyzed by GPC. In both cases, the flow rate of THF through the columns was 1 mL min^{-1}, and samples were filtered before injection into the GPC (filter pore size = 0.45 μm, Albert). Polystyrene standards were used to calibrate the equipment, and for sample analysis, the Mark–Houwink constants of the copolymers were calculated from the values for the homopolymers, taking into account the copolymer composition. The values of the Mark–Houwink[13,14] constants employed are $k_{n\text{-BA}} = 12.2 \times 10^{-3}$ mL/g, $k_{\text{MMA}} = 14.3 \times 10^{-3}$ mL/g, $\alpha_{n\text{-BA}} = 0.7$, and $\alpha_{\text{MMA}} = 0.71$.

The measurement of the MWDs of these nonlinear polymers was not an easy task. To assess the reproducibility of the MWD measurements, GPC analyses were carried out on the sol polymer fraction obtained after the Soxhlet extraction (see Gel Fraction section) and on samples obtained by directly dissolving the latex in THF for an average time of 8 h without agitation at room temperature. The latter method is the one typically used for linear polymer latexes, but without allowing 8 h for dissolution. Figure 3 shows the MWD in terms of elution time for one of the samples (withdrawn at the end of experiment with feed composition 90/10), prepared following both methods. It can be observed that the chromatogram of the sample prepared directly from the

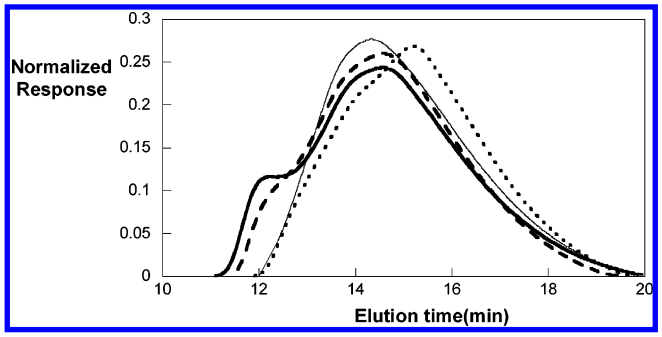

Figure 4. Normalized response versus elution time for the same sample of reaction 90/10, varying the dissolution time: after 8 h (—), after 7days (– – –), after 20 days (– – –), and after Soxhlet extraction (—).

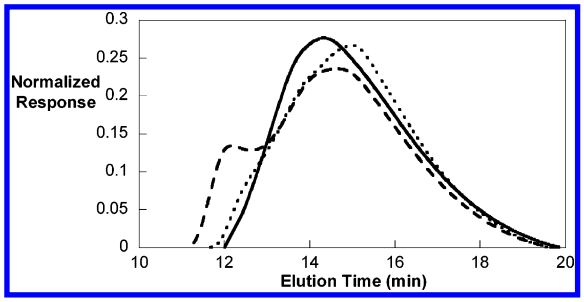

Figure 5. Normalized response versus elution time for a sample from reaction 90/10, after Soxhlet extraction (—), after 1 day of dissolution at 50 °C, (– – –) and after 2 days of dissolution at 50 °C (···).

latex showed a shoulder at low elution times (high molecular weights). This shoulder might be an indication of branched high-molecular-weight chains that are entangled and need more time to reach equilibrium with the solvent. This polymer with high weight-average molecular weight (M_w) was not retained by the filter before the injection into the GPC. However, a latex sample that was left in THF for a weekend showed a smaller shoulder.

The effect of the dissolution time (without agitation) on the measured MWD was studied, and Figure 4 shows that the shoulder disappeared at long dissolution times. This indicates that, because of the branched nature of the samples, it is quite probable that the dissolution process was mass transfer limited;[15] therefore, the longer, more branched chains were entangled, and a long dissolution process was required to disentangle them. Figure 4 shows that about 20 days were needed to dissolve the entangled branched chains and obtain a GPC trace similar to that measured for the soluble fraction from the Soxhlet extraction.

A higher temperature (50 °C) was used in an attempt to reduce the dissolution time. Figure 5 shows that, even after 2 days at 50 °C, the GPC trace showed a small shoulder. The GPC traces of the polymer dissolved during the Soxhlet extraction did not show shoulders because the extraction takes place for 8 h and is performed at high temperature (75 °C) with agitation provided by the continuous reflux of the solvent. An additional advantage of the Soxhlet extraction is that the gel fraction and the sol MWD obtained are for the same sample and, hence, the material balance should be fulfilled. This is not fully guaranteed when the gel fraction is measured by Soxhlet extraction and the sol MWD is determined from the dissolved latex sample.

Mathematical Modeling

A mathematical model developed by Plessis et al.[11] for the homopolymerization of *n*-BA and for the copolymerization of styrene and *n*-butyl acrylate[16] has been used in this work. In this model, radical compartmentalization is considered by the partial distinction approach,[17] and the sol MWD and the gel fraction are calculated using a refined numerical fractionation approach.[18] This refined approach is based on the work by Teymour and Cambell,[19,20] who developed the numerical fractionation approach to calculate the MWD of gel-forming systems in bulk polymerizations.

In the copolymerization of the *n*-BA/MMA system, three types of radicals are involved: (i) a secondary radical on an ultimate unit of type *n*-BA (R_1); (ii) a tertiary (midchain) radical formed by chain transfer to *n*-BA units of the copolymer, both intermolecular and intramolecular (R_2); and (iii) a radical with the ultimate unit of type MMA (R_3). The relevant kinetic mechanisms associated with these radicals (chain transfer to monomer and termination are not included) as included in the present model are detailed in Scheme 1, where $k_{fp1,i}$ is the rate constant for intermolecular chain transfer to polymer of a radical with ultimate unit of type i, $[Q_1]_p$ is the concentration of polymer in the polymerization loci (polymer particles), Y_{BA} is the cumulative copolymer composition referred to *n*-BA, k_{fp2} is the rate constant for intramolecular chain transfer to polymer, $k_{p,ij}$ is the rate constant for propagation of radicals R_i with monomer j, $Y_{BA,inst}$ is the instantaneous copolymer composition referred to *n*-BA, and $[i]_p$ is the concentration of monomer of type i in the polymer particles.

Scheme 1 shows that only R_1 radicals can undergo intramolecular chain transfer to polymer (backbiting), but all three radicals can abstract an H from other BA units in the copolymer chains through intermolecular chain transfer to polymer.

Bimolecular termination in the *n*-BA/MMA comonomer system not only occurs by combination as in the homopolymerization of *n*-BA and copolymerization of *n*-BA with styrene,[11,16] but can also occur by disproportionation because the MMA monomer can terminate by this mechanism.[21] This termination mechanism affects the development of the molecular weight and gel fraction. Thus, the coupling of branched chains that leads

Scheme 1

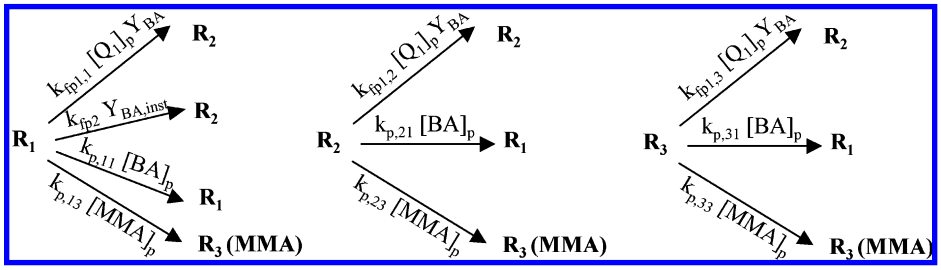

to polymer networks that eventually form gel will be significantly reduced. The terms corresponding to termination by disproportionation that must be added in the balances of the moments of the inactive polymer species are detailed in the Appendix.

The average termination rate constant when no gel effect occurs is computed by the model as follows

$$\bar{k}_{t,0} = k_{t,11}P_1^{\,2} + k_{t,22}P_2^{\,2} + k_{t,33}P_3^{\,2} + 2k_{t,12}P_1P_2 + 2k_{t,13}P_1P_3 + 2k_{t,23}P_2P_3 \quad (2)$$

with

$$k_{t,ij} = (k_{t,ii}k_{t,ij})^{1/2} \qquad \text{and} \qquad k_{t,ij} = k_{t,ji} \quad (3)$$

where $k_{t,ij}$ is the rate constant for termination between radicals of type i and type j. It was assumed that $k_{t,22} = k_{t,33} = k_{t,13} = k_{t,31}$. Each termination rate constant was considered as the sum between the combination ($k_{tc,ii}$) and disproportionation ($k_{td,ii}$) rate constants

$$k_{t,ii} = k_{tc,ii} + k_{td,ii} \quad (4)$$

with

$$k_{tc,ii} = k_{t,ii}C_i \qquad \text{and} \qquad k_{td,ii} = k_{t,ii}(1 - C_i) \quad (5)$$

where C_i is the fraction of termination that occurs by combination of radicals of type i.

In cases where the termination is diffusion controlled (the gel effect is significant), a decrease in the termination rate is observed,[22−24] causing a significant increase in the polymerization rate and a shift in the molecular weight distribution toward higher values. In this case, the average termination rate constant is given by

$$\bar{k}_{t,1} = \bar{k}_{t,0}g \quad (6)$$

where

$$g = \exp\{-[a_1Y_{BA} + a_2(1 - Y_{BA})]\Phi_p^p\} \quad (7)$$

Φ_p^p is the volume fraction of polymer in the polymer particles, and a_1 and a_2 are coefficients (a_1 is related to n-BA and a_2 to MMA).

One must be cautious about the meaning of the experimentally determined gel content to properly consider what gel content is considered by the model. In the present case, gel is considered the polymer fraction that cannot be dissolved in THF (a good solvent of the copolymer). An indication of the minimum molecular weight that cannot be dissolved in THF can be obtained from the GPC trace of the soluble polymer. For these reactions, and as shown in Figures 3−5, no polymer was found over a molecular weight of 1×10^8 g/mol. However, this value should be taken with care because it is in the region where the GPC calibration curve is uncertain. Therefore, the polymer fraction with molecular weights exceeding this value was considered to be gel. Notice that this value is much higher than the one reported by Plessis et al.[11] for n-BA. Therefore, it seems that the comonomer system affects the experimental sol−gel limit of the formed polymer chains. Because the experimental results will be used to fit the model, it is important to implement this criterion in the model to fulfill the sol−gel mass balance measured experimentally.

Table 4. Values of the Kinetic Parameters Taken from the Literature

parameter	value	ref(s)
a_1	2.234	11
C_1, C_2[a]	1.0	11, 32
	0.49	21
r_1, r_2	0.414	33
	2.24	33
k_a^* (dm²/s)	1×10^{-10}	
k_{tW} [L/(mol/s)]	6.55×10^6	11
k_p [L/(mol/s)]		
R_1	40320	34
R_2 ($k_{p,21}$)	40.0	36
R_3	1036	34
$k_{t,0}$ [L/(mol/s)]		
R_1	6.55×10^6	11, 16
R_2	2.0×10^7	34
R_3	2.0×10^7	34
k_{fp1} [L/(mol/s)]		
R_1	0.178	11
R_2	63×10^{-3}	
k_{fp2} (s^{-1})	1470	35

[a] C_i = fraction of termination occurring by combination of radicals of type i.

Parameter Estimation

The mathematical model employed in this work includes many parameters, but some are unavailable in the literature or, in some cases, a very broad range of values is reported. Table 4 contains the values of the parameters taken from the literature. Some parameters remained unknown and were estimated. All of the parameters related to the tertiary (midchain) radical of n-BA are quite uncertain, because little work has been done in this area. Only Plessis et al.[11,25] and Nikitin et al.[26,27] have reported some results for the homopolymerization of n-BA and its copolymerization with styrene.[16] As far as we know, however, nothing has been published about the rate parameters of the tertiary radical of n-BA in n-BA/MMA copolymerization. The following parameters were estimated for the n-BA/MMA system: (i) $k_{p,23}$, the propagation rate constant of the tertiary radicals of n-BA with MMA; (ii) $k_{fp1,3}$, the rate constant for intermolecular chain transfer to polymer of MMA radicals; (iii) a_2, the parameter related to the decrease in the termination rate constant caused by the gel effect due to the presence of MMA; and (iv) k_d^*, the rate constant for radical exit, which was considered to vary with the radius of the swollen polymer particle and the radical concentration in the aqueous phase according to[28]

$$k_d = \frac{k_d^*[R]_w^{\,0.5}}{r_p^{\,1.6}} \quad (8)$$

where k_d^* is considered as an adjustable parameter.

A Nelder−Mead[29] algorithm, based on direct search, was used for parameter estimation (DBCPOL subroutine, IMSL library). The parameters were estimated by fitting model predictions to the experimental data gathered in the seeded semibatch emulsion copolymerizations. The properties taken into account to fit the model predictions to the experimental data were the instantaneous conversion (gravimetry), the gel fraction measured by Soxhlet extraction, and the weight-average

molecular weight of the sol (from GPC measurements of the extracted sol polymer in the Soxhlet process). As mentioned before, by measuring the gel fraction and sol MWD from the same sample, the sol−gel mass balance should be fulfilled (this is not ensured when the GPC samples are prepared directly from the latex). The following objective function was minimized

$$J = \left[\sum_{N} \sum_{n_1(N)} \frac{w_1}{n_1(N)} \left(\frac{x_{\text{inst}_{\text{exp}}} - x_{\text{inst}_{\text{mod}}}}{x_{\text{inst}_{\text{exp}}}} \right)^2 + \sum_{N} \sum_{n_2(N)} \frac{w_2}{n_2(N)} \left(\frac{\text{gel}_{\text{exp}} - \text{gel}_{\text{mod}}}{\text{gel}_{\text{exp}}} \right)^2 + \sum_{N} \sum_{n_3(N)} \frac{w_3}{n_3(N)} \left(\frac{\overline{M}_{\text{wexp}} - \overline{M}_{\text{wmod}}}{\overline{M}_{\text{wexp}}} \right)^2 \right] \quad (9)$$

where N is the number of experiments; w_i represents the weighting factors, $n_i(N)$ is the number of experimental points in each experiment i, and Y_{exp} and Y_{mod} are the experimental and simulated values, respectively, of the variable Y, in this particular case, the instantaneous conversion (x_{inst}), gel fraction (gel), and sol weight-average molecular weight ($\overline{M}_{\text{w}}$). Table 5 presents the estimated values of the adjustable parameters obtained by fitting the model to the experimental results from reaction mixtures with BA/MMA molar compositions of 50/50, 70/30 and 90/10.

Table 5. Values of the Kinetic Parameters Estimated in This Work

parameter	value
$k_{\text{p},23}$ [L/(mol/s)]	68.4
$k_{\text{fp }1,3}$ [L/(mol/s)]	0
a_2	11.2
k_{d}^* (dm^2/s)	5.5×10^{-9}

Results

Figures 6 and 8−10 show the experimental results and the model predictions for the evolutions of the instantaneous conversion and free monomer, cumulative copolymer composition (referred to *n*-BA), gel fraction, and sol weight-average molecular weight, respectively, for the semicontinuous emulsion copolymerizations of BA/MMA using varying monomer ratios. Figure 6a shows that the instantaneous conversion increased as the amount of MMA increased. This trend was also observed for model predictions, giving very good agreement with the experimental data. In all of the reactions, MMA was the first monomer to be consumed (the reactivity ratio of MMA is about 5 times higher than that of *n*-BA), and in the last stages of the reaction (batch period), only *n*-BA was present in the reaction mixture, as can be seen in Figure 6b for the run at the 90/10 monomer ratio. The increase in the instantaneous conversion at higher contents of MMA can be explained by means of the mathematical model. Figure 7a shows the simulated evolution of the average propagation rate coefficient ($\overline{k_{\text{p}}[\text{M}]}$) for reactions with feed compositions of 50/50, 70/30, and 90/10. The highest values correspond to the reaction with the lowest MMA content (90/10), and this does not explain the observed trend in the instantaneous conversion. Figure 7b presents the evolution of the simulated average number of radicals per particle, $\bar{n}$. It can be seen that, as the MMA content increased, the values of $\bar{n}$ also increased and this increase overcame the decrease in $\overline{k_{\text{p}}[\text{M}]}$, yielding an increase of the instantaneous conversion (Figure 6a).

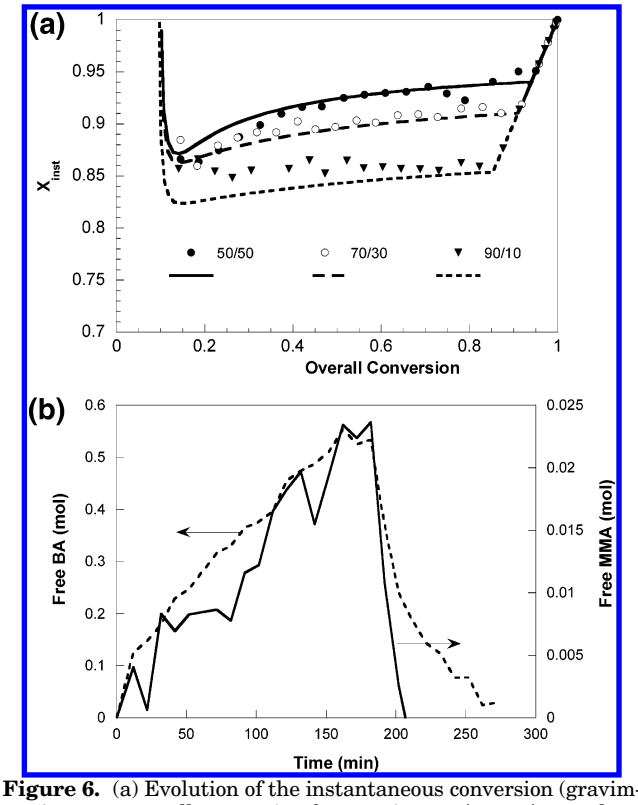

Figure 6. (a) Evolution of the instantaneous conversion (gravimetry) versus overall conversion for reactions 50/50, 70/30, and 90/10 (BA/MMA). Points are experimental data, and lines are model predicitons. (b) Time evolution of the free monomers as measured by on-line Raman spectroscopy for the 90/10 experiment.

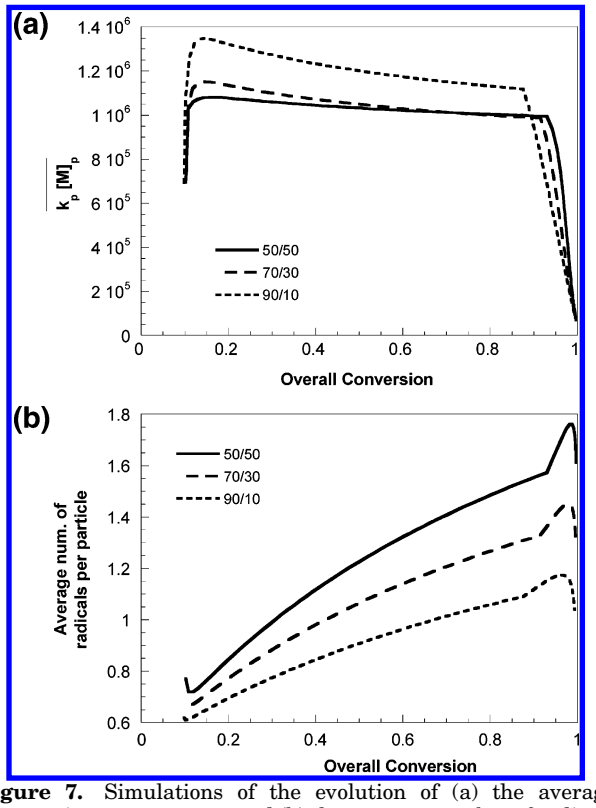

Figure 7. Simulations of the evolution of (a) the average propagation rate constant and (b) the average number of radicals per particle for reactions 50/50, 70/30, and 90/10.

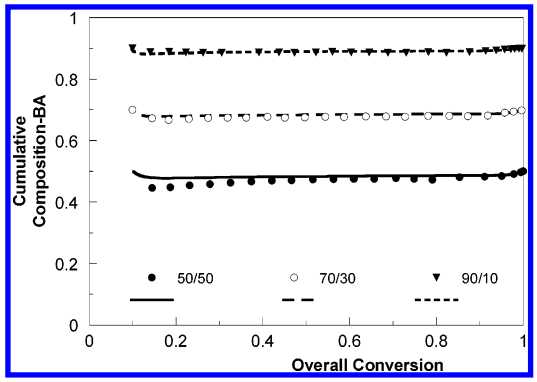

Figure 8. Evolution of the cumulative composition (gas chromatography) based on *n*-BA for reactions 50/50, 70/30, and 90/10. Points are experimental data, and lines are model predictions.

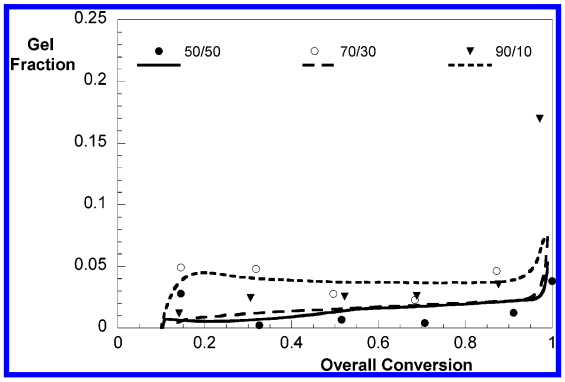

Figure 9. Evolution of the gel fraction for reactions 50/50, 70/30, and 90/10. Points are experimental data, and lines are model predictions.

The reason for the effect of the MMA content on $\bar{n}$ can be found in the average termination rate constant, which, as shown by eqs 6 and 7, is much more strongly affected by the increase of the amount of MMA in the recipe. Note that $a_2 > a_1$, and hence, as Y_{BA} decreases, the decrease of k_t is more pronounced, leading to a higher value of $\bar{n}$.

Figure 8 shows the experimental evolution of the cumulative copolymer composition based on *n*-BA that is well explained by the model predictions. As the reaction proceeds under starved conditions (feeding time was 180 min), the composition for each experiment was quite homogeneous, and the model also predicted this trend.

The evolution of the gel fraction is shown in Figure 9. For all of the reactions, the gel fraction obtained during the semicontinuous stage was low, but the gel fraction increased at the end of the reaction, during the batch time, when no more monomer was being added into the reactor. Figure 9 shows that the gel content increased with the BA content in the monomer mixture. The experimental data were well explained by the model. Several factors made the gel fraction decrease as the content of MMA in the feed composition increased. It is worth pointing out that homopolymerizations of BA under the same semibatch conditions yield 60% gel polymer.[9,11,25] In this system, gel is formed by the combination of intermolecular chain transfer to polymer (that leads to long chain branches in the polymer) and termination by combination of branched growing radicals (leading to network formation and eventually gel polymer). Because H abstraction occurs in BA units,[11,30,31] the increase of MMA units in the copolymer chains reduces the option of having branched

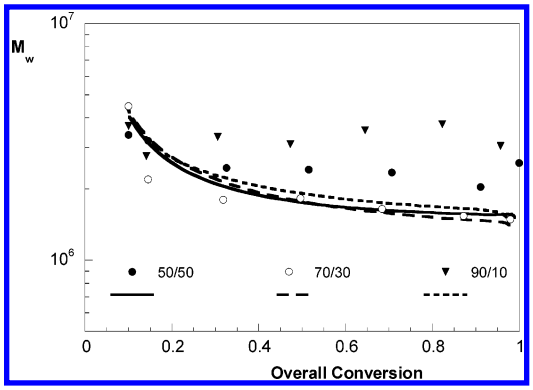

Figure 10. Evolution of the sol weight-average molecular weight for reactions with BA/MMA feed compositions 50/50, 70/30, and 90/10. Points are experimental data, and lines are model predictions.

radicals. Furthermore, in copolymerization, the MMA monomer is more reactive than the BA monomer (see Table 4), and hence, the predominant radical species are in MMA units, whose activity for hydrogen abstraction is significantly lower. In the same vein, MMA radicals do terminate by disproportionation, which also reduces the probability of having cross-linking branched chains and, hence, gel polymer formation. At the end of the reaction, during the batch period, there was an increase in the gel content that was well predicted by the model. At this stage, only *n*-BA was present in the reactor (see Figure 6b); therefore, chain transfer to polymer increased because of the higher polymer concentration and the relative abundance of secondary radicals. In addition, termination occurred mainly by combination. This led to long branched chains that, after coupling by termination by combination, formed polymer networks that eventually led to gel.

The evolution of the sol weight-average molecular weight, $\overline{M_w}$, is depicted in Figure 10. Experiments show that the amount of MMA did not have a clear effect on the sol $\overline{M_w}$. According to the model, higher sol $\overline{M_w}$ values would be produced at lower MMA contents, although the expected effect was modest. However, this effect of the amount of MMA on the sol $\overline{M_w}$ was not observed in the experimental data. The highest sol $\overline{M_w}$ values corresponded to reaction 90/10 (with the lower MMA content), as was predicted by the model, but the experimental values were higher than those predicted by the model. For reaction 70/30, with an intermediate MMA content, a much better agreement was obtained between experimental and predicted values. For reaction 50/50, the experimental values of the sol $\overline{M_w}$ were higher than the predicted ones. It might be possible (the open literature has few reports on sol molecular weight and gel content measurements in gel-forming copolymerization systems[7,8,10]) that this discrepancy is due to the limitations of the size-exclusion chromatographic technique when dealing with high-M_w, long, nonlinear, branched polymer solutions.

Concluding Remarks

The kinetics and polymer microstructure (composition, gel fraction, and sol molecular weight) of high-solids-content (50 wt %) seeded *n*-BA/MMA emulsion copolymerization reactions were investigated in this work. The data were analyzed by means of a mathematical model. The kinetics, copolymer composition,

and gel fraction were well predicted by the model, but discrepancies arose in attempts to fit the sol $\overline{M}_w$. The measurement of the sol MWD for these nonlinear polymers using gel permeation chromatography is not an easy task. As shown in Figures 3−5, the high-molecular-weight tails of the GPC traces lie on the boundaries of the range in which the calibration can be considered reliable, and hence, the molecular weights reported are uncertain. This might be the reason for the model mismatch.

Acknowledgment

O.E. acknowledges Ministerio de Educación y Ciencia for the scholarship. The authors acknowledge the financial support from the University of the Basque Country (Grant UPV 00221.215-13594/2001) and CICYT (Project PP02000-1185).

Appendix: Moments of the Chain Length Distributions of Dead Polymer

The balances for the kth-order moments of the overall chain length distribution of the dead polymer in generation n, $Q_k(n)$, can be expressed as the sums of the contributions of each of the processes, s, leading to the formation of dead polymer in the particles containing different numbers of radicals, i

$$\frac{dQ_k(n)}{dt} = \sum_s \sum_{i=1}^{m} \frac{dQ^i_{k,s}(n)}{dt} \qquad \text{(A-1)}$$

The kth-order moments of the chain length distribution of dead polymer produced by the different mechanisms can be found in ref 16 except for that produced by the mechanism of disproportionation, which can be expressed as follows

Termination by disproportionation

$$\frac{dQ^i_{k,\mathrm{td}}(n)}{dt} = \overline{c_{\mathrm{td}}}(j-1)[p^i_k(n) + q^i_k(n)] \qquad \text{(A-2)}$$

where $p^i_k(n)$ and $q^i_k(n)$ are the kth-order moments of the length distributions of radicals p and q, respectively, belonging to a general nth generation, with

$$\overline{c_{\mathrm{td}}} = \frac{\overline{k_{\mathrm{t},0}}(d)g}{N_A v_p} \quad \text{and} \quad \overline{c_{\mathrm{tc}}} = \bar{c} - \overline{c_{\mathrm{td}}} \qquad \text{(A-3)}$$

and $\overline{k_{\mathrm{t},0}(d)}$ calculated from the homotermination rate constants and the probabilities of having the ultimate unit of each type of radical

$$\overline{k_{\mathrm{t},0}(d)} = k_{\mathrm{t},11}(d)P_1^2 + k_{\mathrm{t},22}(d)P_2^2 + k_{\mathrm{t},33}(d)P_3^2 + 2k_{\mathrm{t},12}(d)P_1P_2 + 2k_{\mathrm{t},13}(d)P_1P_3 + 2k_{\mathrm{t},23}(d)P_2P_3 \qquad \text{(A-4)}$$

$$k_{\mathrm{t},ij}(d) = k_{\mathrm{t},ji}(d) = [k_{\mathrm{t},ii}(d)k_{\mathrm{t},jj}(d)]^{1/2} \qquad \text{(A-5)}$$

Literature Cited

(1) Urban, D.; Distler, D. In *Polymer Dispersions and their Industrial Applications*; Urban, D., Takamura, K., Eds.; John Wiley & Sons: New York, 2002; Chapter 1, p 1.

(2) Dubé, M. A.; Penlidis, A. A Systematic Approach to the Study of Multicomponent Polymerization Kinetics: Butyl Acrylate/Methyl Methacrylate/Vinyl Acetate. III. Emulsion Homopolymerization and Copolymerization in a Pilot Plant Reactor. *Polym. Int.* **1995**, *37*, 235.

(3) Chern, C. S.; Hsu, H. Semibatch Emulsion Copolymerization of Methyl Methacrylate and Butyl Acrylate. *J. Appl. Polym. Sci.* **1995**, *55*, 571.

(4) Novak, R. W. Mechanism of acrylic emulsion polymerizations. *Adv. Org. Coat. Sci. Technol. Ser.* **1988**, *10*, 54.

(5) Ouzineb, K.; Fortuny Heredia, M.; Graillat, C.; McKenna, T. F. Stabilization and Kinetics in the Emulsion Copolymerization of Butyl Acrylate and Methyl Methacrylate. *J. Appl. Polym. Sci. A: Polym. Chem.* **2001**, *39*, 2832.

(6) Britton, D. J.; Lovell, P. A.; Heatley, F.; Venkatesh, R. Chain Transfer to Polymer in Emulsion Copolymerizations. *Macromol. Symp.* **2001**, *175*, 95.

(7) Sayer, C.; Lima, E. L.; Pinto, J. C.; Arzamendi, G.; Asua, J. M. Kinetics of the Seeded Semicontinuous Emulsion Copolymerization of Methyl Methacrylate and Butyl Acrylate. *J. Polym. Sci. A: Polym. Chem.* **2000**, *38*, 367.

(8) Sayer, C.; Lima, E. L.; Pinto, J. C.; Arzamendi, G.; Asua, J. M. Molecular Weight Distribution in Composition Controlled Emulsion Copolymerization. *J. Polym. Sci. A: Polym. Chem.* **2000**, *38*, 1100.

(9) Plessis, C. Modeling of Molecular Weight Distribution of Polyacrylic Latexes in Seeded Semicontinuous Emulsion Polymerization. Ph.D. Dissertation, University of the Basque Country, San Sebastián, Spain, 2001.

(10) Malihi, F. B.; Kuo, C. Y.; Provder, T. Determination of Gel Content of Acrylic Latexes by Size Exclusion Cromatorgraphy. *J. Liq. Chromatogr.* **1983**, *6*, 667.

(11) Plessis, C.; Arzamendi, G.; Leiza, J. R.; Schoonbrood, H. A. S.; Charmot, D.; Asua, J. M. Modeling of Seeded Semibatch Emulsion Polymerization on *n*-Butyl Acrylate. *Ind. Eng. Chem. Res.* **2001**, *40*, 3883.

(12) Elizalde, O.; Leiza, J. R.; Asua, J. M. On-line Monitoring of All-Acrylic Emulsion Polymerization Reactors by Raman Spectroscopy. *Macromol. Symp.* **2004**, *206*, 135.

(13) Beuermann, S.; Paquet, D. A., Jr.; McMinn, J. H.; Hutchinson, R. A. *Macromolecules* **1996**, *29*, 4206.

(14) Vicente, M. Control optimo de la producción de polímeros en emulsión en base a medidas calorimétricas. Ph.D. Dissertation, University of the Basque Country, San Sebastián, Spain, 2001.

(15) van Krevelen, D. W. *Properties of Polymers*; Elsevier: Amsterdam, 1990.

(16) Plessis, C.; Arzamendi, G.; Leiza, J. R.; Schoonbrood, H. A. S.; Charmot, D.; Asua, J. M. Kinetics and Polymer Microstructure of the Seeded Semibatch Emulsion Copolymerization of *n*-Butyl Acrylate and Styrene. *Macromolecules* **2001**, *34*, 5147.

(17) Arzamendi, G.; Sayer, C.; Zoco, N.; Asua, J. M. Modeling of MWD in Emulsion Polymerization: Partial Distinction Approach. *Polym. React. Eng.* **1998**, *6*, 193.

(18) Arzamendi, G.; Asua, J. M. Modeling Gelation and Sol Molecular Weight Distribution in Emulsion Polymerization. *Macromolecules* **1995**, *28*, 7479.

(19) Teymour, F.; Campbell, J. *Numerical Fractionation—A Novel Technique for the Mathematical Modelling of Long Chain Branching and Cross-linking in Polymer Systems*; DECHEMA Monograph 127; DECHEMA: Frankfurt am Main, Germany, 1992.

(20) Teymour, F.; Campbell, J. Analysis of the Dynamics of Gelation in Polymerization Reactors Using the "Numerical Fractionation" Technique. *Macromolecules* **1994**, *27*, 2460.

(21) Schulz, G. V.; Henrici-Oliveé, G.; Olivé, S. Determination of Absolute Velocity Constants for the Chain Growth and the Two Chain-Breaking Reactions, Disproportionation and Combination in Methyl Methacrylate. *Z. Phys Chem.* **1960**, *27*, 1.

(22) Friis, N.; Hamielec, A. E. Note on the Kinetics of Methyl Methacrylate Emulsion Polymerization. *J. Polym. Sci. A: Polym. Chem.* **1974**, *12*, 251.

(23) Friis, N.; Hamielec, A. E. Gel Effect in Emulsion Polymerization of Vinyl Monomers. In *Emulsion Polymerization*; Piirma, I., Gardon, A., Eds.; Academic Press: New York, 1976.

(24) Lee, C. F.; Chiu, W. E.; Chern, Y. C. Kinetic Study on the Poly(methyl methacrylate) Seeded Soapless Emulsion Polymerization of Styrene. II. Kinetic model. *J. Appl. Polym. Sci.* **1995**, *57*, 591.

(25) Plessis, C.; Arzamendi, G.; Leiza, J. R.; Schoonbrood, H. A. S.; Charmot, D.; Asua, J. M. A Decrease in Effective Acrylate Propagation Rate Constants Caused by Intramolecular Chain Transfer. *Macromolecules* **2000**, *33*, 4.

(26) Nikitin, A. N.; Castignolles, P.; Charleux, B.; Vairon, J.-P. Determination of Propagation Rate Coefficient of Acrylates by Pulsed Laser Polymerization in the Presence of Intramolecular Chain Transfer to Polymer. *Macromol. Rapid Commun.* **2003**, *24*, 778.

(27) Nikitin, A. N.; Castignolles, P.; Charleux, B.; Vairon, J.-P. Simulation of Molecular Weight Distribution Obtained by Pulsed Laser Polymerization (PLP): New Analytical Expressions Including Intramolecular Chain Transfer to the Polymer. *Macromol. Theory Simul.* **2003**, *12*, 440.

(28) Asua, J. M. A New Model for Radical Desorption in Emulsion Polymerization. *Macromolecules* **2003**, *36*, 6245.

(29) Nelder, J. A.; Mead, R. A Simplex Method for Function Minimization. *Comput. J.* **1964**, *7*, 308.

(30) Lovell, P. A.; Shah, T. H.; Heatley, F. Correlation of the Extent of Chain Transfer to Polymer Reaction Conditions for Emulsion Polymerization of *n*-Butyl Acrylate. In *Polymer Latexes: Preparation, Characterization, and Applications*; Daniels, E. S., Sudol, E. D., El-Aasser, M. S., Eds.; ACS Symposium Series No. 492; American Chemical Society: Washington, DC, 1992.

(31) Peck, A.; Hutchinson, R. A. Secondary Reactions in the High-Temperature Free Radical Polymerization of Butyl Acrylate. *Macromolecules* **2004**, *37*, 5944.

(32) Moad, G.; Solomon, D. H. *The Chemistry of Free Radical Polymerization*; Elsevier Science: New York, 1995.

(33) Hutchinson, R. A.; MacMinn, J. H.; Paquet, D. A.; Beuermann, S.; Jackson, C. A Pulsed-Laser Study of Penultimate Copolymerization Propagation Kinetics for Methyl Methacrylate/*n*-Butyl Acrylate. *Ind. Eng. Chem. Res.* **1997**, *36*, 1103.

(34) Beuermann, S.; Buback, M. Rate Coefficients of Free-Radical Polymerization Deduced from Pulsed Laser Experiments. *Prog. Polym. Sci.* **2002**, *27*, 191.

(35) Plessis, C.; Arzamendi, G.; Alberdi, J. M.; van Herk, A. M.; Leiza, J. R.; Asua, J. M. Evidence of Branching in Poly(*n*-butyl acrylate) produced in pulsed laser polymerization experiments. *Macromol. Rapid Commun.* **2003**, *24*, 173.

(36) Arzamendi, G.; Plessis, C.; Leiza, J. R.; Asua, J. M. Effect of the Intramolecular Chain Transfer to Polymer on PLP−SEC Experiments of Alkyl Acrylates. *Macromol. Theory Simul.* **2003**, *12*, 315.

Received for review February 26, 2004
Revised manuscript received September 8, 2004
Accepted September 8, 2004

IE0400649